

# Quasi-periodic spin chains in a magnetic field

M. Arlego<sup>1</sup>, D.C. Cabra<sup>1,2</sup> and M.D. Grynberg<sup>1</sup>

<sup>1</sup>*Departamento de Física, Universidad Nacional de La Plata, C.C. 67, (1900) La Plata, Argentina.*

<sup>2</sup>*Facultad de Ingeniería, Universidad Nacional de Lomas de Zamora, Cno. de Cintura y Juan XXIII, (1832), Lomas de Zamora, Argentina.*

We study the interplay between a (quasi) periodic coupling array and an external magnetic field in a spin- $\frac{1}{2}$   $XXZ$  chain. A new class of magnetization plateaux are obtained by means of Abelian bosonization methods which give rise to a sufficient quantization condition. The investigation of magnetic phase diagrams via exact diagonalization of finite clusters finds a complete agreement with the continuum treatment in a variety of situations.

PACS numbers: 71.10.Fd, 71.10.Pm, 75.60.Ej.

The magnetic properties of quasi-crystals have become a fundamental issue of study since their discovery in 1984 [1]. A variety of theoretical efforts, ranging from renormalization group (RG) analysis of Ising models in Penrose lattices [2] to exact solutions of both Ising and  $XY$  Fibonacci spin chains [3–5] have revealed fairly intricate magnetic orderings associated to the quasi-periodicity of these structures. The non-metallic spin exchange mechanism implicit in those studies has been evidenced in recently synthesized rare earth ( $\mathcal{R}$ )  $ZnMg\text{-}\mathcal{R}$  quasi-crystals (see *e.g.* [6]) whose  $\mathcal{R}$  elements have well localized  $4f$  magnetic moments.

Bolstered by these latter findings and as a further step within the line of the local moment descriptions referred to above, here we consider the ordering of quasi-periodic spin- $\frac{1}{2}$   $XXZ$  chains in a magnetic field to elucidate the quantization conditions of massive spin excitations or magnetization plateaux. In periodic systems, this issue has received systematic attention in the last few years from both experimental and theoretical points of view (see *e.g.* [7]). In this letter, we are specifically interested in studying the antiferromagnetic system

$$H_{qp} = J \sum_n (1 + \epsilon_n) (S_n^x S_{n+1}^x + S_n^y S_{n+1}^y + \Delta S_n^z S_{n+1}^z) - h \sum_n S_n^z, \quad (1)$$

where  $S^x, S^y, S^z$  denote the spin- $\frac{1}{2}$  matrices involved in the standard  $XXZ$  Hamiltonian ( $\epsilon_n = 0$ ) in a magnetic field  $h$  applied along the anisotropy direction ( $|\Delta| \leq 1$ ). Here, the coupling modulation is introduced via the  $\epsilon_n$  parameters defined as  $\epsilon_n = \sum_\nu \delta_\nu \cos(2\pi \omega_\nu n)$ , so quasi-periodicity arises upon choosing an irrational subset of frequencies  $\omega_\nu$  with amplitudes  $\delta_\nu$ .

The interest of (1) stems partly from the widespread applications of  $1d$  Hamiltonians in the description of artificially grown quasi-periodic heterostructures [8], quantum dot crystals [9] and magnetic multilayers [10]. Also, recent investigations of quasi-periodicity involving either the couplings [11] or the magnetic field [12], have been addressed using Abelian bosonization along with RG and

numerical techniques. Here we focus on the combined effect of a quasi-periodic exchange modulation under a uniform magnetic field.

Of particular importance are the rational frequencies of (1), not only as a way to approach the quasi-periodic limit, but also because they allow for a thorough numerical verification of a novel situation (see [13–15] for related work). As we shall see, although the allowed fractional plateaux predicted in the present case fall into the classification provided by the generalized Lieb-Schultz-Mattis theorem [16], a bosonization approach to (1) yields an alternative scenario not envisaged in previous studies [17,18]. This will be reflected in the appearance of magnetization plateaux associated to each of the frequencies present in (1). To strengthen the potential interest of our results, we show how a simple two frequency model exhibits a magnetization curve with two wide plateaux at  $1/4$  and  $3/4$  of saturation, a situation which is highly reminiscent of that observed in magnetization experiments on  $NH_4CuCl_3$  [19].

Following the standard bosonization procedure (see *e.g.* [20]), the continuum limit of the  $XXZ$  Hamiltonian in the presence of an external magnetic field  $h$  is given by the Tomonaga-Luttinger Hamiltonian

$$H = \frac{1}{2} \int dx \left( vK (\partial_x \tilde{\phi})^2 + \frac{v}{K} (\partial_x \phi)^2 \right). \quad (2)$$

The bosonic field  $\phi$  and its dual  $\tilde{\phi}$  are given by the sum and difference of the light-cone components, respectively. The constant  $K = K(\langle M \rangle, \Delta)$  governs the conformal dimensions of the bosonic vertex operators and can be obtained exactly from the Bethe Ansatz solution of the  $XXZ$  chain (see *e.g.* [18] for a detailed summary). One has  $K = 1$  for the  $SU(2)$  symmetric case ( $\Delta = 1$ ) and it is related to the radius  $R$  of [18] by  $K^{-1} = 2\pi R^2$ . In terms of these fields, the spin operators read

$$S_x^z = \frac{1}{\sqrt{2\pi}} \partial_x \phi + a : \cos(2k_F x + \sqrt{2\pi} \phi) : + \frac{\langle M \rangle}{2}, \quad (3)$$

$$S_x^\pm = (-1)^x : e^{\pm i\sqrt{2\pi}\tilde{\phi}} \left( b \cos(2k_F x + \sqrt{2\pi}\phi) + c \right) :, \quad (4)$$

where the colons denote normal ordering with respect to the ground state with magnetization  $\langle M \rangle$ . The Fermi momentum  $k_F$  is related to the magnetization of the chain as  $k_F = (1 - \langle M \rangle)\pi/2$ . Either the  $XXZ$  anisotropy or an external magnetic field modify the scaling dimensions of the physical fields through  $K$  and the commensurability properties of the spin operators, as can be seen from (3), (4). The non-universal constants  $a$ ,  $b$  and  $c$  can be in general computed numerically (see *e.g.* [21], for the case of zero magnetic field) and in particular the constant  $b$  has been obtained exactly in [22].

For the sake of clarity, let us first consider the effect introduced by a *single* frequency term in Eq. (1), i.e.  $\epsilon_n = \delta \cos(2\pi\omega n)$ . Thus, using Eqs. (3) and (4) it follows that the relevant part of the interaction term in  $H_{qp} = H + H_{int}$  reads

$$H_{int} = \sum_x \cos(2\pi\omega x) \left[ \lambda_1 (\partial_x \tilde{\phi})^2 + \lambda_2 (\partial_x \phi)^2 + \lambda_3 \cos(2k_F x + \sqrt{2\pi}\phi) + \lambda_4 \sin(2k_F x + \sqrt{2\pi}\phi) \right] \quad (5)$$

where  $\lambda_i \propto \delta$ ,  $i = 1, \dots, 4$ .

As in previous analysis [16–18] one can readily obtain the necessary quantization condition for the appearance of a plateau by looking at the commensurability of the relevant operators. In the present case we need only to consider the vertex operators  $\exp \pm i\sqrt{2\pi}\phi$  of scaling dimension  $d = 1/(4\pi R^2)$ . Therefore, we obtain that  $\langle M \rangle$  should satisfy

$$\langle M \rangle = \pm(2\omega - 1), \quad (6)$$

in order for a plateau to be present. The fulfillment of this condition opens a spin gap excitation since the operator in question is relevant at least for  $0 < \Delta < 1$ . In the region  $-1 < \Delta < 0$  a critical curve appears which can be determined from the Bethe-Ansatz solution for  $R(\langle M \rangle, \Delta)$  [18]. Furthermore, the gap width can be easily computed to scale as  $\delta^{1/(2-d)}$ . Notice that the perturbations  $\lambda_{1,2}$  do not play a role here since they are incommensurate whenever (6) holds.

In fact, these expectations turn out to apply well above the weak coupling regime discussed so far. In Fig. 1 we show the magnetization phase diagram resulting from exact diagonalization of fairly large  $XX$  chains ( $10^5$  spins) by setting  $\omega = 13/21$  through a wide range of couplings. Notice that for rational frequencies,  $\omega \in \mathcal{Q}$  and  $\delta \rightarrow \delta_c$ , for some appropriate value of  $\delta_c$  which depends on  $\omega$ , the chain breaks up into a periodic collection of *finite* segments which naturally yield additional plateaux of rational values. Being the unit cell composed of 21 spins one would naively expect plateaux to appear for values of  $M = (2n + 1)/21$ ,  $n = 0, \dots, 10$ , but as can be seen from Fig. 1 this is not the case due to the non-trivial structure of the unit cell and only some of these values are indeed observed. Interestingly, Eq. (6) yet remains robust all the way through the decoupling point and the corresponding plateau corresponds to the most prominent.

These observations were also corroborated on  $XXZ$  chains. However, owing to the large spaces involved in their diagonalization now we content ourselves with moderate lengths  $L$  (up to 24 spins). After resorting to the Lanczos method [23] in each of the magnetization subspaces with  $S^z \in \{0, 1, \dots, L/2\}$ , we built up the magnetization contours shown in Fig. 2 using  $\omega = 5/8$  for  $L = 8, 16, 24$ . As expected, the massless  $XXZ$  excitations around  $\langle M \rangle = 1/4$  render size effects rather noticeable within small coupling regions. Nevertheless, already for  $\delta > 0.2$  they clearly become less pronounced, thus lending our results further support to the bosonization picture.

A word of caution should be added here, namely, the importance of periodic boundary conditions (PBC) in testing the analytic approach via exact diagonalization of small systems. Already at the level of a simple dimerized chain ( $\omega = 1/2$ ), PBC become crucial. In fact, the numerical analysis of this latter situation using *open* boundary conditions shows that the well known  $\langle M \rangle = 0$  plateau expected in the large length  $L$ -limit, actually emerges at  $\langle M \rangle = 2/L$ . Fig. 3 illustrates this observation for  $L = 24, 20$  and 16 and should emphasize the essential role of PBC in all our subsequent numerical checks.

By construction, the bosonization approach can be straightforwardly extended to the case in which more than one frequency is present in  $\epsilon_n$ . It turns out that whenever condition (6) is satisfied *for each frequency*, a magnetization plateau shows up. This extension is simple since each operator (corresponding to each frequency) is commensurate separately, and hence the different perturbations can be treated separately. Of course the situation changes in the case of a dense multi-frequency spectrum (such as in the Fibonacci potential that we discuss below) and a more complete analysis has to be carried out [11].

In order to test the reliability of these predictions, we have analyzed numerically both  $XX$  and  $XXZ$  chains using double-frequency couplings. In Fig. 4 we display the magnetization curves obtained for  $\omega_1 = 5/8$ ,  $\omega_2 = 7/8$  with amplitudes  $\delta_1 = 0.2$  and  $\delta_2 = 0.3$  respectively. As we mentioned before, the rather robust plateaux emerging at  $\langle M \rangle = 1/4$  and  $3/4$  not only confirm the correctness of our extended bosonization prediction, but also pave the way to an alternative description of the massive spin excitations observed in  $\text{NH}_4\text{CuCl}_3$ ; a quasi-one-dimensional  $S = \frac{1}{2}$  compound which is attracting both theoretical and experimental attention and whose magnetization behavior yet remains unexplained [19,24,25]. Of course, a more realistic description of this material must start from the microscopic structure observed by X-ray spectroscopy, which points to a two-leg zigzag ladder. Still, it is quite encouraging to obtain a magnetization curve qualitatively similar with the simple two-frequency model we considered here.

In studying irrational frequencies or other quasi-periodic modulations, it is natural to check our analysis with the prototype Fibonacci sequence, a coupling array

$J_A = J(1 + \delta)$ ,  $J_B = J(1 - \delta)$  generated by iterating the substitution rules  $B \rightarrow A$  and  $A \rightarrow AB$  [3-5,11]. Here we discuss the general  $XXZ$  situation (a related model has been studied in [26]), and compare our results with the already well known magnetization curve of the  $XX$  case [4,5]. Before continuing with the bosonization approach, we pause to discuss the *strong* coupling regimes of this system ( $\delta \rightarrow \pm 1$ ) in the context of a simple decimation procedure (see *e.g.* [27]). To evaluate the magnetization of the widest plateaux, there are two different cases to consider, according to  $\delta \simeq -1$ , i.e.  $J_B \gg J_A$ , and the opposite situation for  $\delta \simeq 1$ .

Starting from saturation, in the first case the magnetic field is lowered until it reaches the value  $h_c \simeq J_B$  at which the type- $B$  bonds experience a transition from the state of maximum polarization to the singlet state. The magnetization at this plateau is then obtained by decimating the  $B$  bonds. This simply yields  $\langle M \rangle = 1 - 2N_B/(N_B + N_A)$ , where  $N_{A,B}$  denotes the number of bonds of type  $A$  and  $B$  respectively. For a large iteration number of the rules referred to above ( $L \rightarrow \infty$ ),  $N_A/N_B$  approaches the golden mean  $\gamma = (1 + \sqrt{5})/2$  and therefore we find  $M_1 = (\gamma - 1)/(\gamma + 1) \simeq 0.236068$ .

In the second case,  $J_A \gg J_B$ , we have to distinguish two different unit cells since type- $A$  bonds can appear either in pairs (forming trimers) or isolated (forming dimers). It can be readily checked that when lowering the magnetic field from saturation the first spins to be decimated correspond to those forming trimers. We then find two plateaux at  $M_2 = 1 - 2/\gamma^3 \simeq 0.527864$  (after decimating trimers) and, alike the case  $\delta \simeq 1$ , at  $M_1$  (after decimating the remaining dimers). Since the decimation procedure applies for generic  $XXZ$  chains [27], we conclude that the emergence of these strong coupling plateaux is a generic feature, at least with an antiferromagnetic anisotropy parameter  $0 < \Delta < 1$ .

For intermediate regimes  $0 < |\delta| < 1$  the magnetization curve has a much richer structure which can be easily understood from our bosonization analysis in a multi-frequency case. Evidently, the self similar hierarchy of frequencies resulting from the Fourier transform of the Fibonacci exchanges (see *e.g.* [11]) along with the quantization condition studied so far, enables to reconstruct the whole spin gap structure of the Fibonacci chain, at least for  $|\delta| \ll 1$  and as long as the operator responsible for the plateaux is relevant. Actually, it turns out that one can obtain a fair approximation to the latter showing the most important plateaux by keeping just a few number of main spectrum frequencies, even beyond weak coupling regimes. Interestingly, when the constraint (6) is applied to the dominant Fibonacci frequencies  $\omega_1 = 1/\gamma$  and  $\omega_2 = 2(1 - 1/\gamma)$ , it yields precisely the  $M_1$  and  $M_2$  plateaux arising from the strong coupling decimation. These results are shown in Fig. 5 where both single and double-frequency approximations are displayed. Moreover, using the Fourier spectrum to set  $\delta_2/\delta_1 \simeq 0.36237$ , the Fibonacci gap widths exhibit a remarkable agreement

with the scaling exponents  $1/(2 - d)$  referred to above. This can be observed in the inset over more than three decades in  $\delta$ . In turn, this supports the observation that *all* gap widths of the  $XX$  Fibonacci chain scale simultaneously with  $\delta$ , as for  $\Delta = 0$  the compactification radii comprehended in the scaling exponents are independent of the magnetization [ $R \equiv 1/(2\sqrt{\pi})$ ] (see *e.g.* [18]).

Finally, we point out that for the Fibonacci chain (which has a dense Fourier spectrum), it was shown by solving the one-loop RG equations at zero magnetic field [11] (see also [12]) that the critical value of  $R$  at which the Kosterlitz-Thouless transition occurs is moved to  $R_c = 1/\sqrt{4\pi}$ , in contrast to  $R_c = 1/\sqrt{8\pi}$  for the single, or more generally non-dense frequency case. Hence, for  $0 < \Delta < 1$  and arbitrary magnetization, the operator responsible for spin gap openings at each of the Fibonacci frequencies is relevant. Therefore, the magnetization curve of the  $XXZ$  case with antiferromagnetic anisotropy is of the same form as that of the  $XX$  situation (see Fig. 5), though with different plateaux widths.

To summarize, we have studied the interplay between quasi-periodic exchanges and uniform magnetic fields in strongly correlated antiferromagnetic chains using both bosonization and numerical techniques. The former were tested and complemented by the latter in a variety of non-perturbative scenarios. Our calculations suggest the possibility to observe rather stable magnetization plateaux [Eq. (6)] on artificially grown arrays of quantum dots [9] according to the (controlled) spatial distribution of their exchange integrals. We trust this work will convey an interesting motivation for further experimental studies in these material technologies.

It is a pleasure to acknowledge useful discussions with A. Honecker and P. Pujol. The research of D.C.C and M.D.G. is partially supported by CONICET and Fundación Antorchas, Argentina (grant No. A-13622/1-106).

- 
- [1] D. Schechtman, I. Blech, D. Gratias and J.W. Cahn, Phys. Rev. Lett. **53**, 1951 (1984).
  - [2] C. Godrèche, J.M. Luck and H. Orland, J. Stat. Phys. **45**, 777 (1986).
  - [3] Y. Achiam, T.C. Lubensky and E.W. Marshall, Phys. Rev. B **33**, 6460 (1986).
  - [4] J.M. Luck and Th.M. Nieuwenhuizen, Europhys. Lett. **2**, 257 (1986).
  - [5] M. Kohmoto, B. Sutherland and C. Tang, Phys. Rev. B **35**, 1020 (1987).
  - [6] T.J. Sato, H. Takakura, A.P Tsai, K. Shibata, K. Ohoyama and K.H. Andersen, Phys. Rev. B **61**, 476 (2000).
  - [7] D.C. Cabra, M. D. Grynberg, A. Honecker and P. Pujol, preprint cond-mat/0010376.
  - [8] R. Merlin, K. Bajema, R. Clarke, F.-Y. Juang and P.K.

- Bhattacharya, Phys. Rev. Lett. **55**, 1768 (1985)
- [9] L. P. Kouwenhoven, F.W.J. Hekking, B.J. van Wees, C.J.P.M. Harmans, C.E. Timmering and C.T. Foxon, Phys. Rev. Lett. **65**, 361 (1990).
- [10] C.G. Bezerra, J.M. de Araujo, C. Chesman and E.L. Albuquerque, preprint cond-mat/0101099.
- [11] J. Vidal, D. Mouhanna and T. Giamarchi, Phys. Rev. Lett. **83**, 3908 (1999).
- [12] K. Hida, Phys. Rev. Lett. **86**, 1331 (2001); K. Hida, J. Phys. Soc. Jpn. **68** (1999) 3177; *ibid.* **69**, Suppl. A, 311 (2000).
- [13] W. Chen, K. Hida and H. Nakano, J. Phys. Soc. Jpn. **68**, 625 (1999).
- [14] R.M. Wießner A. Fledderjohann, K.-H. Mütter and M. Karbach, Eur. Phys. J. B **15**, 475 (2000).
- [15] O. Derzhko, J. Richter and O. Zaburannyi, J. Magn. Magn. Matter **222**, 207 (2000).
- [16] M. Oshikawa, M. Yamanaka and I. Affleck, Phys. Rev. Lett. **78**, 1984 (1997).
- [17] K. Totsuka, Phys. Lett. **A228**, 103 (1997).
- [18] D.C. Cabra, A. Honecker and P. Pujol, Phys. Rev. Lett. **79**, 5126 (1997); Phys. Rev. B **58**, 6241 (1998).
- [19] H. Tanaka, K. Takatsu, W. Shiramura, T. Kambe, H. Nojiri, T. Yamada, S. Okubo, H. Ohta and M. Motokawa, Physica B **246**, 545 (1998); W. Shiramura, K. Takatsu, B. Kurniawan, H. Tanaka, H. Uekusa, Y. Ohashi, K. Takizawa, H. Mitamura, T. Goto, J. Phys. Soc. Jpn. **67**, 1548 (1998).
- [20] A.O. Gogolin, A.A. Nersesyan and A.M. Tsvelik, *Bosonization of Strongly Correlated system* (Cambridge University Press, Cambridge, England 1998).
- [21] T. Hikihara and A. Furusaki, Phys. Rev. B **58**, R583 (1998).
- [22] S. Lukyanov and A. Zamolodchikov, Nucl. Phys. B **493**, 571 (1997).
- [23] Consult for example G.H. Golub, C.F. Van Loan, “*Matrix Computations*”, 3rd edition (Johns Hopkins University Press, Baltimore 1996).
- [24] A.K. Kolezhuk, Phys. Rev. B **59**, 4181 (1999).
- [25] D.C. Cabra and M.D. Grynberg, Phys. Rev. B **62**, 337 (2000).
- [26] T. Tokihiro, Phys. Rev. B **41**, 7334 (1990).
- [27] D.C. Cabra, A. De Martino, M. D. Grynberg, S. Peysson and P. Pujol, Phys. Rev. Lett. **85**, 4791 (2000); ; D.S. Fisher, Phys. Rev. B **50**, 3799 (1994); S.K. Ma, C. Dasgupta and C.-K. Hu, Phys. Rev. Lett. **43**, 1434 (1979); C. Dasgupta and S.K. Ma, Phys. Rev. B **22**, 1305 (1979).

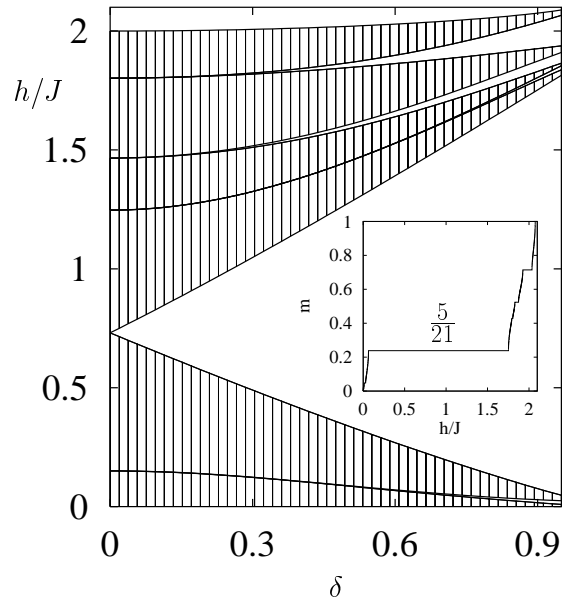


FIG. 1. Critical fields (in bold lines) of the  $XX$  chain with  $\omega = 13/21$  and  $10^5$  spins. At  $\delta = 0.9$  these fields conform the standard magnetization curve displayed in the inset. Vertical lines denote regions of massless spin excitations where the magnetization increases continuously with  $h$ . Empty zones in ascending order represent plateaux appearing at  $\langle M \rangle = 1/21, 5/21$  [central region expected by Eq. (6)],  $9/21, 11/21$  and  $15/21$  before saturation (top zone).

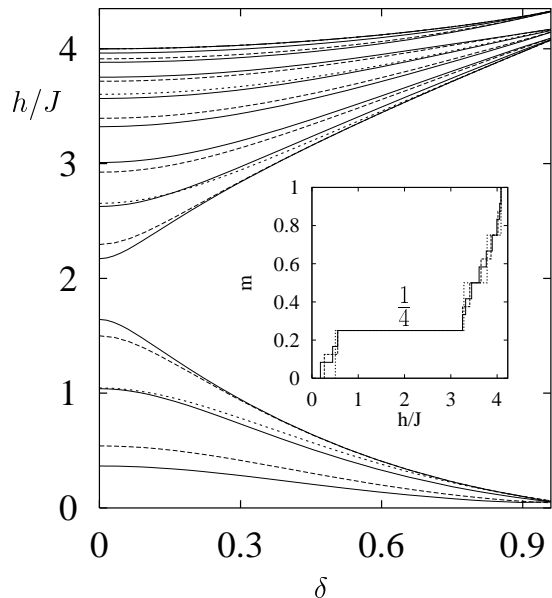


FIG. 2. Magnetization contours of the isotropic ( $\Delta = 1$ )  $XXZ$  chain for  $\omega = 5/8$ . Solid, dashed and dotted lines stand respectively for the critical fields of  $L = 24, 16$  and  $8$ . The middle empty region corresponds to the  $\langle M \rangle = 1/4$  plateau expected by Eq. (6). The inset shows one of the typical magnetization curves upon setting  $\delta = 0.5$ .

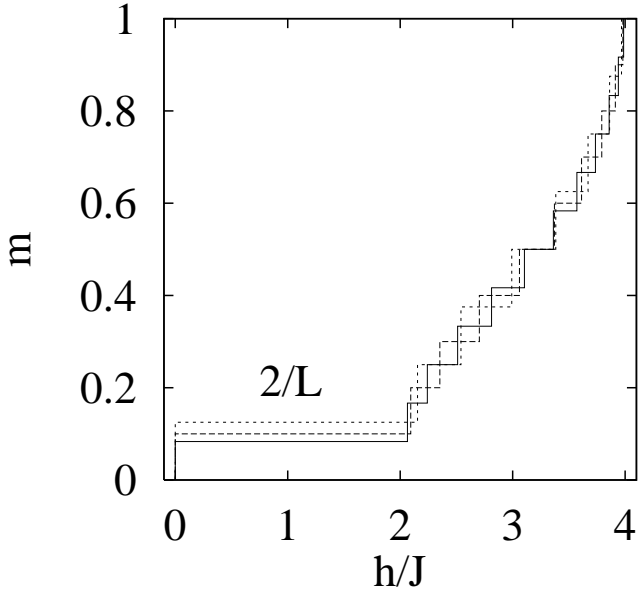


FIG. 3. Magnetization curves of a dimerized Heisenberg chain ( $\omega = 1/2$  with  $\delta = 0.4$ ), using *open* boundary conditions displaying a plateau at  $\langle M \rangle = 2/L$ . Solid, dashed and dotted lines denote respectively the results of  $L = 24, 20$  and  $16$ .

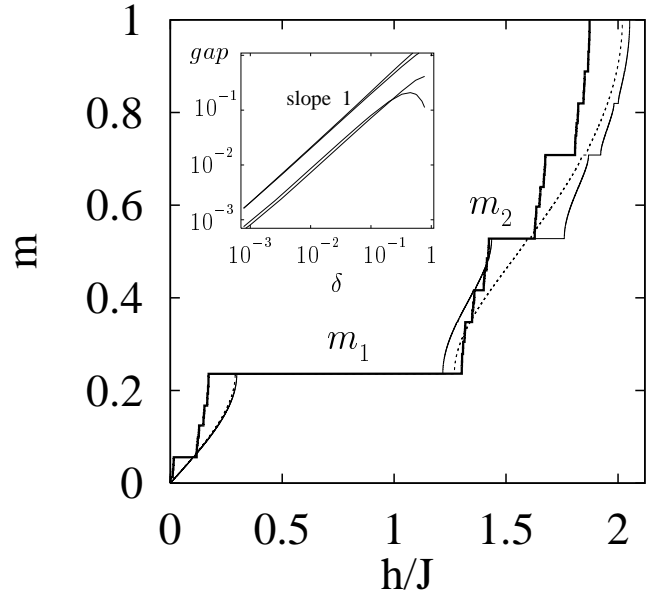


FIG. 5. Fibonacci magnetization for  $\delta = 0.5$  and  $F(25) = 75025$   $XX$  spins (bold line). Here,  $F(25)$  denotes the  $25^{\text{th}}$  Fibonacci number defined as  $F(n+1) = F(n) + F(n-1)$  with  $F(1) = F(2) = 1$ . Dotted and solid lines stand respectively for the single and double frequency approximants to the  $M_1$  and  $M_2$  plateaux referred to in the text. The slopes compared in the inset show the gap width of  $M_2$  and  $M_1$ , in ascending order. Bold lines denote the Fibonacci gaps whereas solid lines represent the double approximant widths.

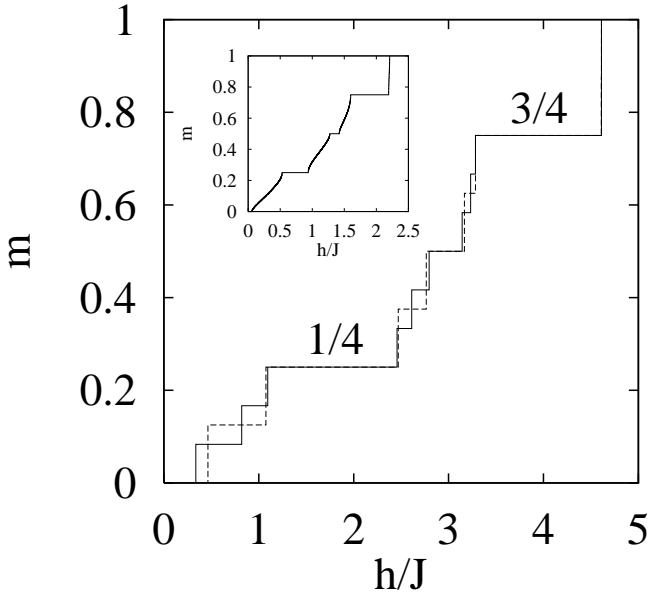


FIG. 4. Double frequency magnetization curve of the isotropic ( $\Delta = 1$ )  $XXZ$  chain for  $\omega_1 = 5/8, \omega_2 = 7/8$  with amplitudes  $\delta_1 = 0.2$  and  $\delta_2 = 0.3$ . Solid and dashed lines denote respectively the magnetizations of  $L = 24$  and  $16$ . The inset shows the magnetization curve of the corresponding  $XX$  chain with  $10^5$  spins.